Slow Down Dewetting in Polymer Films by Isocyanate-treated Graphite Oxide

Pei Bai,Hua Li

[c] *University of Michigan-Shanghai Jiao Tong University Joint Institute, Shanghai Jiao Tong University, Shanghai 200240, China*

Abstract Isocyanate-treated graphite oxides (*i*GOs) were well-dispersed into the polystyrene (PS) thin films and formed a novel network structure. With control in fabrication, an *i*GOs-web layer was horizontally embedded near the surface of the films and thus formed a composite slightly doped by *i*GOs. This work demonstrated that the *i*GOs network can remarkably depress the dewetting process in the polymer matrix of the composite, while dewetting often leads to rupture of polymer films and is considered as a major practical limit in using polymeric materials above their glass transition temperatures (T_g). *Via* annealing the 50–120 nm thick composite and associated neat PS films at temperatures ranging from 35 °C to 70 °C above T_g, surface morphology evolution of the films was monitored by atomic force microscopy (AFM). The *i*GOs-doped PS exhibited excellent thermal stability, *i.e.*, the number of dewetting holes was greatly reduced and the long-term hole growth was fairly restricted. In contrast, the neat PS film showed serious surface fluctuation and a final rupture induced by ordinary dewetting. The method developed in this work may pave a road to reinforce thin polymer films and enhance their thermal stability, in order to meet requirements by technological advances.

Keywords Dewetting; Thin polymer films; Thermal instability; *i*GOs network

INTRODUCTION

Ultra-thin polymer films have a variety of applications ranging from lubricants, adhesives, protective coatings to photovoltaics and dielectric layers, but the films' dewetting and the resultant rupture have long been obstacles for their practical use[1−12]. In past several decades, investigations on instability of supported thin polymer films have attracted great attention; among these studies, effort on polymer nanocomposite has been devoted[13−17]. With the addition of nanofillers such as silica nanoparticles[18], fullerene[19−22], carbon nanotubes[23, 24], and recently polymer-grafted gold nanoparticles[25, 26], properties of the polymer nano-composites can be improved in mechanical strength and thermal resistance, *via* altering polymer behavior by the nanofiller's intrinsic properties and/or introducing desired interfacial interactions[13, 27]. However, the nanofiller's poor dispersity and technological complex are still the barriers toward high-performance nanocomposites.

As a potential nanofiller, graphene—a typical two-dimensional (2D) nanoplatelet nowadays reliably obtained from the resourceful graphite oxides—has been utilized with bulk polymers to improve the dielectric, mechanical as well as thermal properties[25−28]. Furthermore, the unique nanostructure and excellent properties make graphene an ideal filling material for ultra-thin films, but due to the challenges in sheet exfoliation and dispersion of the nanoplatelets, synergizing these materials in ultra-thin polymer films remains problematic. However, the advantages of 2D graphene derivatives are certain: geometrically the 2D materials work cooperatively with films especially when thickness is reduced, and the mobility and dewetting could be depressed if a network of the 2D filler is formed in the polymer film[29]. Here, we developed a novel nanocomposite to improve ultra-thin film stability, that is, firstly thinning the graphite oxide (GO) by organic isocyanate[30, 31], then attaining an uniform web-like isocyanate-treated graphite oxides (*i*GOs) *via* spin-coating from a solution. On this basis, we fabricated the web-like *i*GOs with thickness of 10–15 nm and dissolved them into thin polystyrene (PS) films. After annealing the film well above the bulk PS's glass transition temperature (T_g, 106 °C, measured by a differential scanning calorimeter in the second heating) for a long time, it is found that the dewetting phenomenon[1, 2] has been prominently depressed in the composites. To the best of our knowledge, this is the first time to fabricate *i*GOs web into thin polymer films with both

well-controlled morphology and dispersion, and simultaneously obtain excellent improvement in thermal stability.

EXPERIMENTAL

Materials

N,*N*-dimethylformamide (DMF) (> 99.8%, anhydrous) and graphite oxide (> 99%) were purchased from Aladdin Company at Shanghai, China. The graphite oxide was dried over phosphorus pentoxide in a vacuum oven for a week before use. Polystyrene (PS, M_w = 280 kg/mol and PDI = 1.02) was purchased from Sigma-Aldrich. Dimethyl phenyl isocyanates (M_w = 135.7 g/mol) and organic solvents such as toluene and methylene chloride were purchased from Sinopharm Chemical Reagent Co, Ltd. If not specified, the materials and chemicals above were used as received without any further purification or treatment.

Processing of the Graphite Oxides

The graphite oxides were thinned following a typical process of chemical exfoliation by using organic isocyanates[30, 31]. Firstly, 10 mg of pre-dried GO was put into a 10-mL round bottom flask and then 1 mL of anhydrous DMF was added under nitrogen protection. Subsequently, 0.5 mmol of organic isocyanate, which was kept in liquid at 50 °C prior to use, was slowly dropped into the flask. The resulting mixture was stirred at room temperature for 24 h, and turned into a slurry-like matter and exhibited grey color with small black fragments suspended in the liquid. The treated GO solution was then added drop by drop into methylene chloride (10 mL) for coagulation, followed by further filtering and washing by additional methylene chloride (20 mL). Finally, the product, isocyanate-treated graphite oxides (*i*GOs), was dried under vacuum at 35 °C for 12 h.

Isocyanate-treated graphite oxides (5 mg) prepared above was added into anhydrous DMF (5 mL) in a 10-mL vial and fully dissolved by mild ultrasonic exfoliation for 1 h. Thus a stable dispersion of *i*GOs in DMF was formed, and the organic solvent also maintained a good dissolving capacity for polymers like polystyrene. Then the *i*GOs solution was dropped on a silicon wafer with a native oxide layer, which was rinsed by deionized water prior to use, and then dried in air at room temperature overnight. To examine the morphology of *i*GOs on the substrate, topological images of the film were taken by a Bruker Fast-Scan atomic force microscope (AFM) under non-contact tapping mode. A representative topological image with *i*GOs fragments coiled and twisted was observed, which was generated directly from drop cast of *i*GOs solution in DMF, as shown in Fig. 1(a). To achieve a well-dispersed *i*GOs atop a silicon wafer with a native oxide layer or PS film, the *i*GOs-DMF solution was mixed with pure toluene in a volume ratio 2:1 or 3:1, and hence the mixture exhibited a good solubleness for *i*GOs as well as an enhanced volatility in spin coating process. Fig. 1(b) shows the typical spin-coating result from the *i*GOs solution in DMF and toluene, which is a novel web-like structure. This well-dispersed *i*GOs web exhibited a continuously connected network with nearly no fragments piling up; and the cross-section line in Fig. 1(c) also shows a relatively uniform *i*GOs-web, with profile height varying from 10 nm to 15 nm.

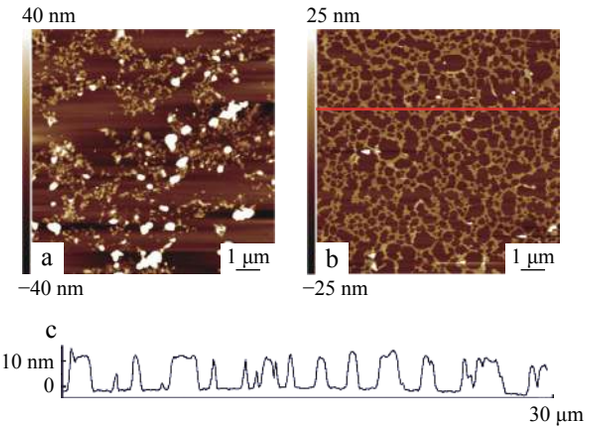

Fig. 1 AFM images showing *i*GOs morphology on silicon wafer with a native oxide layer. (a) *i*GOs in DMF was dropped on the substrate. (b) *i*GOs in DMF-toluene mixture was spin-coated on the substrate. (c) Corresponding *i*GOs web height profile along the red section line in panel (b).

Fabrication of the Composite Film

To form a thin layer of *i*GOs-web atop a PS film, first, a PS (M_w = 280 kg/mol) film, was prepared by spin-coating (The spinning speed was 2000 r/min). Subsequently, the existing film and substrate were kept rotating at the same speed, while a little dosage of *i*GOs-DMF-toluene mixture (3–10 μL) was dropped down to the center of the film through a hole of the cover of the spin coater. During this process, the organic solvents (toluene and DMF) in the mixture quickly dissolved the PS film near free surface while the *i*GOs simultaneously expanded within a top layer due to the spin, and thus a thin layer of *i*GOs/PS composite was formed in the PS film.

Fig. 2 displays this process, and especially Fig. 2(c) shows the schematic of the final product. The solid gray area is the neat PS film with no impact in the process of *i*GOs-web coating, which shows a relatively flat and uniform morphology in AFM images, compared with a fluctuated one for the composite area showed in Fig. 2(d). This obvious surface fluctuations within ± 3 nm is further displayed in the 3D AFM image, and along the red line, the height profile represents the morphology from the interaction between the *i*GOs-web and its polymer host. What should be mentioned is that the matrix should be kept relatively thick, usually no less than 50 nm, to ensure a better *i*GOs-web layer fabrication. The thicknesses of both neat PS film and the area with composite were nearly the same, proven by AFM test as well as the same color shown in optical microscopy.

RESULTS AND DISCUSSION

Dewetting for the Composite Films

To examine the fluidity of *i*GOs-doped PS films, the samples were annealed at 141, 156, and 176 °C, *i.e.*, 35–70 °C above the T_g of the bulk PS, at various time intervals. After annealing, the samples were quenched to room temperature and stored in a humidity-controlled box at −4 °C. The

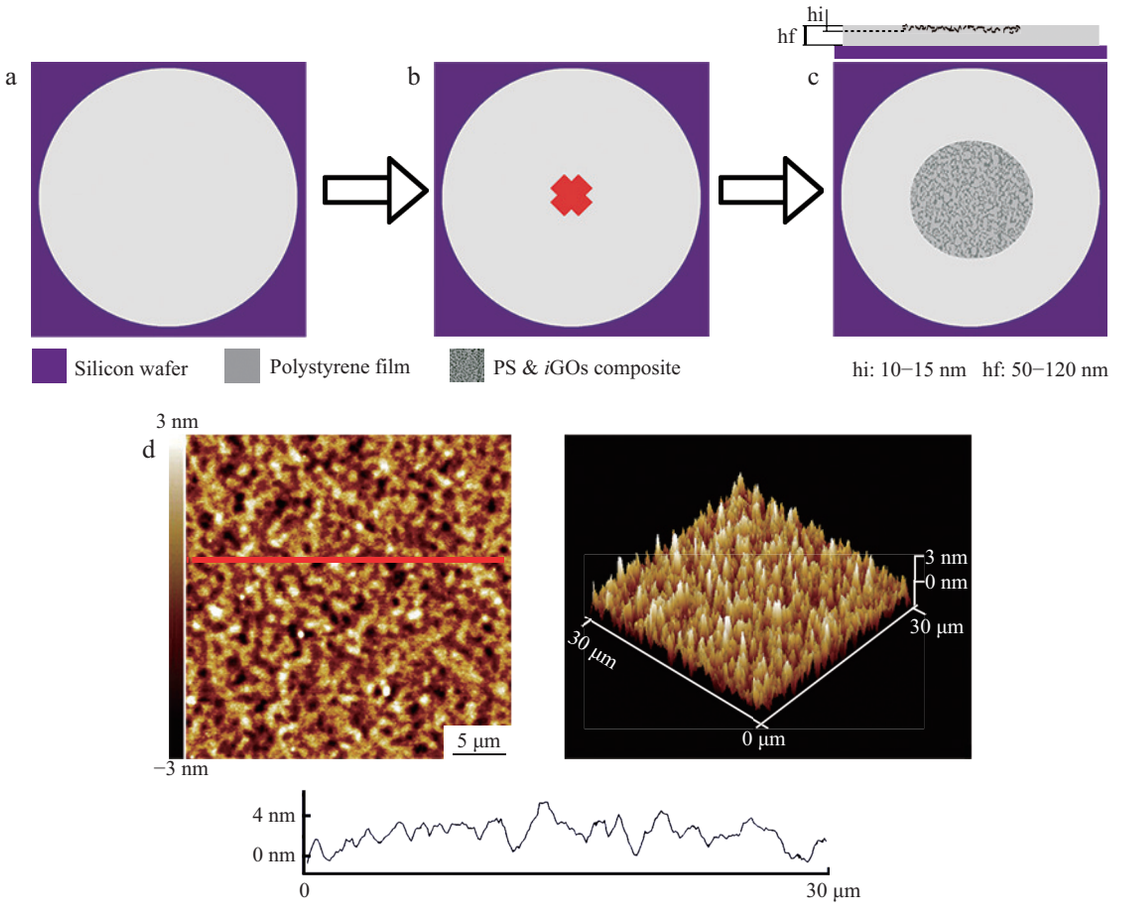

Fig. 2 Preparation process of *i*GOs/PS composite film. (a) Neat PS was spin-coated on silicon wafer with a native oxide layer. (b) The *i*GOs mixture was dropped on the film center. (c) Schematic of the final composite product, with *i*GOs scattering in the film center around and the outside edge still being neat PS. (d) Topography of the composite surface by AFM.

morphology of each sample, as response of its thermal stability, was measured by AFM. Fig. 3 presents a series of representative AFM topological images of *i*GOs-doped PS films of 72-nm thick, annealed at 156 °C. For a direct comparison, the morphology of neat PS films in control experiments is displayed as well. In contrast to the neat PS film that showed the typical dewetting features including holes' opening and growth, the *i*GOs-doped PS films presented high resistance of holes' nucleation, opening, and enlargement. In the neat PS film, holes were nucleated within 5 min, and then underwent a continuous growing process, with surroundings evidently fluctuating, as shown in Fig. 3(a). Consistent with the mechanism of large-scale surface mobility[32], at this temperature, dewetting holes of neat PS films broadened remarkably, as observed in many previous studies[1−3, 5, 6]. The *i*GOs-doped area exhibited neither much surface fluctuation (represented by roughness of the AFM images) like neat PS, nor pervasively hole nucleation and continuous growth. As illustrated in Fig. 3(b), at the early stage of annealing the remnants of uniform web morphology from *i*GOs network gradually disappeared due to diffusion of PS molecules and the film remained relatively flat surface. Moreover, the dewetting process of PS was dramatically depressed by the *i*GOs network, which was confirmed by tracking a representative area of the composite film and monitoring the hole diameter change.

Although the holes also nucleated within 5 min as shown in Figs. 3(b) and 3(c), they underwent totally different growing process from ordinary dewetting. Firstly, the growth rate of hole diameter of *i*GOs-doped PS film was much lower than that of the neat material, which implied that the dewetting process could be driven to start as usual, but further hole growth was greatly constrained by the filled *i*GOs layer. Secondly, in the *i*GOs/PS composite, the diameter of dewetting hole could either increase or decrease in the annealing process, deviated vastly from ordinary dewetting. This indicated that the *i*GOs web influenced the mass transfer of the macromolecules and therefore the dewetting holes were kept small over the whole film in the entire timescale of annealing test.

Holes Featured in the Composite Zone

Fig. 4 depicts the hole profile evolution versus annealing time. In the experimental timescale, both the hole depth and diameter of *i*GOs-doped PS increased with a lower pace than those in neat PS. An example is shown in Figs. 4(a) and 4(b). The dewetting holes with the same radius of ~1 μm at the initial point of observation were found deepening vertically and expanding horizontally at quite different rates. As a

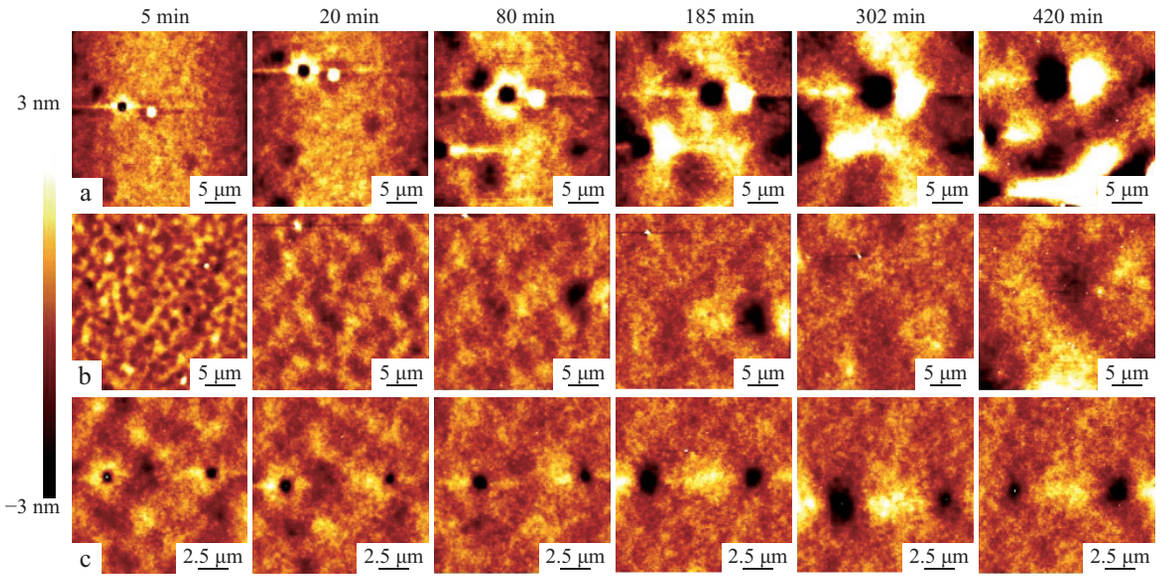

Fig. 3 Dewetting test for neat PS and the composite in the same film. The result was obtained for a 72-nm-thick PS (M_w = 280 kg/mol) film at 156 °C, 50 °C above its bulk T_g. (a) is captured from the neat PS while (b) is from the composite, and (c) is the hole-emerging zone captured in the composite area. The scale bar for (a) and (b) is 5 μm while it is 2.5 μm for (c).

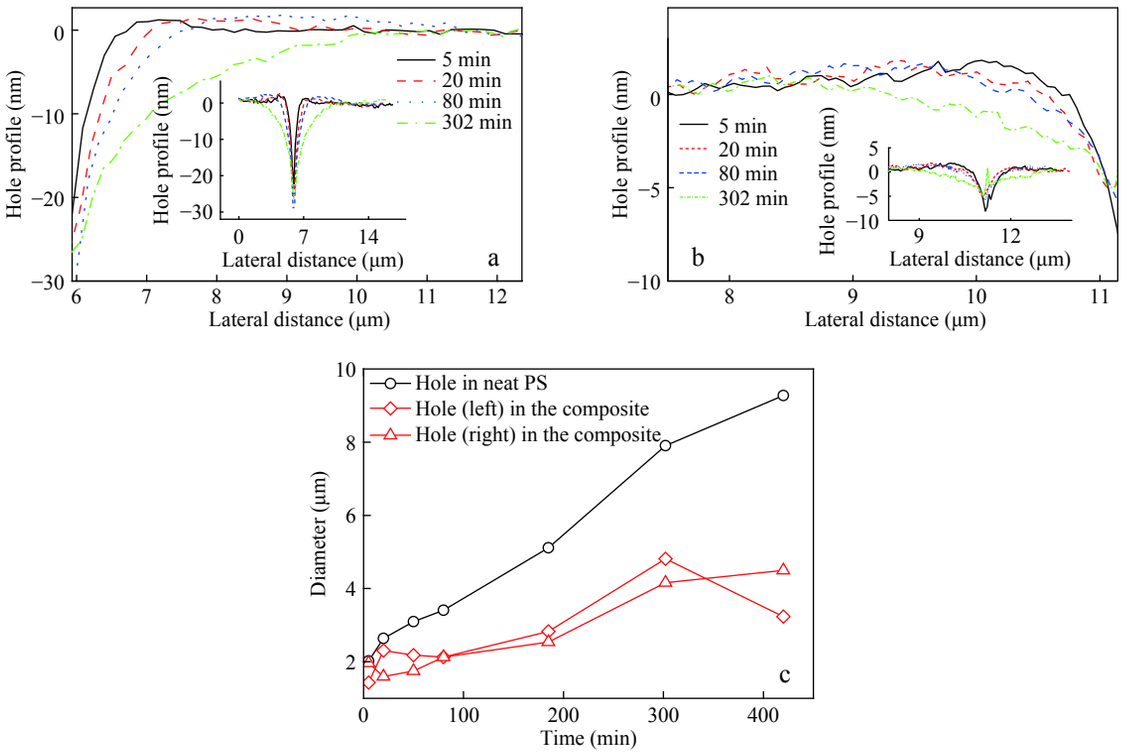

Fig. 4 (a, b) The growing profiles of holes found in neat PS and the composite area respectively, corresponding to holes in panels (a) and (c) of Fig. 3. The insets are the intact growing section of each part. (c) The holes' diameter evolution.

result, the size of dewetting hole in neat PS was approximately triple in depth and double in diameter of that in the *i*GOs-doped PS after annealing at 156 °C for 302 min.

Apparently, the uniform connected *i*GOs could generate enormous interfacial area and greatly affect the fluidity and stability of the surrounding polymer matrix at temperatures well above T_g. Due to large increase in molecular interfaces between the matrix and the *i*GOs sheets, the entropically-unfavorable web-like morphology was believed to be maintained even going through high-temperature annealing for a long time[16, 17], during which the connected *i*GOs sheets could physically act as a stumbling block, as proven by the quite slow hole opening as well as hole narrowing and restoring shown in Fig. 3(c). Despite the interaction between the *i*GOs layer and the substrate due to their mutual attraction[8], the wholly connected web was believed hard to

move downward even at the presence of continuous coverage of surrounding polymers. This probably originated mainly from the capillary waves-induced surface fluctuations[9], and inversely this process leveled the film surface and prohibited hole nucleation and growth as shown in Figs. 3(b) and 3(a), respectively. Moreover, this novel density fluctuation-integrated *i*GOs web may not cause the common surface destabilization[10, 33]. As such, the stabilization of thin polymer films from dewetting was achieved by embedding small amount of thin *i*GOs web layer in the polymer, enabling the latter's behavior affected by both surface mobility[32] and interfacial effect with *i*GOs. Besides, functionalized graphite oxide treated by isocyanate[30, 31] still retained many functional groups, including epoxy groups and hydroxyl groups in the sheet center and carbonyl/carboxyl groups at the edge[28] as well as the reacted residuals containing orthogonal functionalities such as cyano, keto, and azidosulfonyl[30]. Whether these functional groups have played a critical role in providing strong interfacial interaction with the host polymer and thus leading to a long-time stabilization of the material, will be investigated in the future.

Fig. 5 presents the boundary of a dewetting hole in the composite film with its thickness of 83 nm, at 141 °C (T_g + 35 °C) for 15 min. As shown in Fig. 5(a), an AFM height image illustrates that the hole merged into its vicinity smoothly, that is, the ordinary accumulated rim surrounding a dewetting hole did not appear in the *i*GO-doped PS film. This result reflects the unique dewetting features shown in this work, *i.e.*, the mobility of polymer might be enhanced by the embedded *i*GOs as well, so the excess mass from hole opening and growth could propagate into the main body of the film rapidly. The inset (left) shows the morphology in a larger scale, compared to a hole boundary in neat PS (right) at the same time. Additionally, the 3D AFM image detailed the unique topography of the hole in the composite, while the simultaneously dewetting holes in neat PS exhibited ordinary surrounding rim, driven by capillary force between the polymer and the substrate. In neat PS the holes grew faster and caved deeper than those in the composite, which had a depth of only 3 nm at most in the PS under confinement reinforced by *i*GOs network.

All of the herein evidence shows that the floating *i*GOs web can work as an effectively preventing filler against the dewetting of ultra-thin film, which has long proven a fierce phenomenon upon high temperature and is believed to be a critical preventing factor for dewetting[1, 2, 11, 32].

Dewetting for Composites with *i*GOs Slightly-embedded

To clearly show the *i*GOs structure in the composite, the network was made partially protuberant from the PS surface. This was achieved by adjusting the spinning speed when *i*GOs was capped upon. The resulting composite with its thickness of 98 nm also showed excellent thermal stability. Fig. 6 presents the results from a two-stage annealing test: first at a temperature of 141 °C for 68 min, and then at 176 °C for 100 min. Fig. 6(a) displays the initial composite film surface captured by AFM, showing *i*GOs frame in the network merging into the polymer matrix. And in Fig. 6(b), optical images of the composite film (left) and the neat PS film (right) exhibit the resulting morphologies from depressed and ordinary dewetting after annealing, respectively. Here the insets show the representative surface topography for both the composite and neat PS. In Fig. 6(b), the *i*GOs frames are looming when continuous matrix polymer being covered on them; nearly no permanent dewetting holes are detected, apparently different from the neat PS, and such large-scale stability is also found in other composite films.

Fig. 6(c) shows the overall surface roughness. Before annealing, the composite film had a much rougher surface as shown in Fig. 6(a) due to the near surface *i*GOs network; during the first step of annealing, at 35 °C above T_g, the composite film flattened quickly; then in the high-

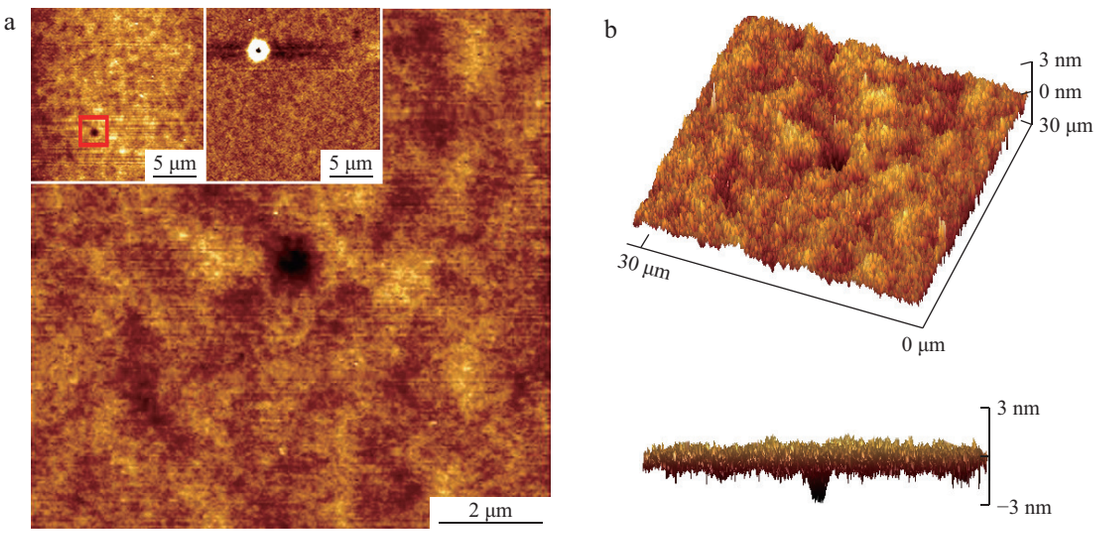

Fig. 5 An example of dewetting hole emerging in the composite surface. (a) AFM height image shows a dewetting hole in the composite zone. The inset (left) is the hole in a larger scale, compared with another hole (right inset) simultaneously appearing in neat PS zone. (b) 3D AFM image shows detail on the boundary of the dewetting hole, without surrounding rim observed.

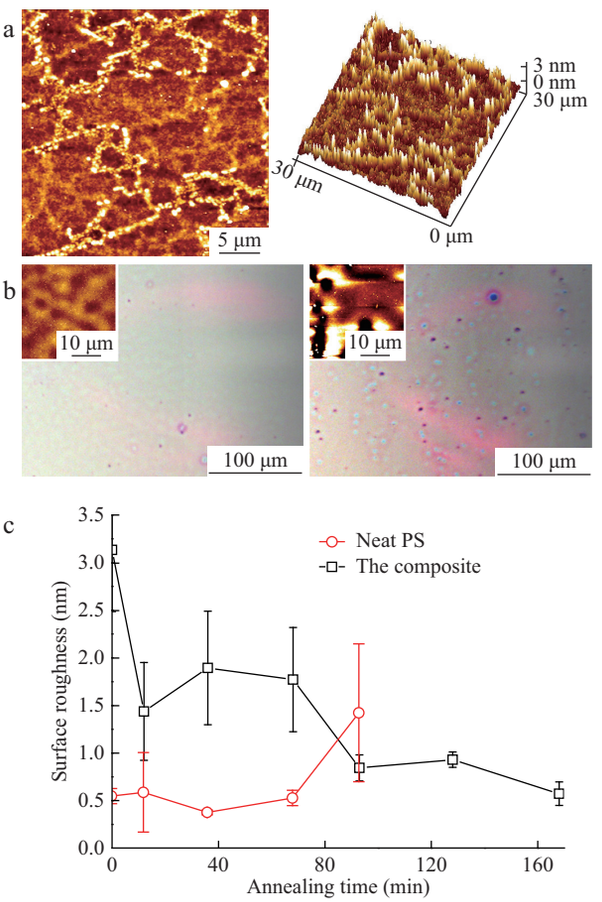

Fig. 6 Annealing of the composite film with higher *i*GOs concentration. (a) AFM height pictures for the composite film before annealing, with obvious web-like *i*GOs floating on. The right picture gives the corresponding 3D image. (b) Optical pictures show the morphology for the composite film (left) and neat PS film (right) after annealed at 141 °C for 68 min firstly and then at 176 °C for 25 min. The insets exhibit representative resultant morphology by AFM. (c) The surface roughness evolution during annealing. The films experienced the temperature protocol as mentioned in the text, and the roughness of neat PS is not available after 100 min due to film rupture. The error bars represent standard deviation.

temperature annealing process (T_g + 70 °C) for 20 min, the composite film experienced a slow but continuous flattening process while the neat PS film showed a large-scale rupture at the beginning of this stage and formed droplets when annealing went on.

CONCLUSIONS

In summary, we coated the isocyanate-treated graphitic nanoplatelets on ultra-thin PS films, thus forming well-dispersed *i*GOs networks near the free surface. After annealing at high temperature, it was found that the composite film exhibited an evidently different fluidity, and dewetting was remarkably prohibited in the composite film due to the existence of the uniform *i*GOs network, while in the corresponding neat PS film, hole opening, growth, and fierce rupturing were observed in the same timescale. The way of slightly embedding the *i*GOs into PS film could provide a general approach to improve the thermal stability of thin polymer films in their applications for state-of-the-art technologies, and definitely, the generality of this approach needs to be extensively further studied.

REFERENCES

1 Reiter, G. Dewetting of thin polymer films. Phys. Rev. Lett. 1992, 68(1), 75.
2 Xie, R.; Karim, A.; Douglas, J. F.; Han, C. C.; Weiss, R. A. Spinodal dewetting of thin polymer films. Phys. Rev. Lett. 1998, 81(6), 1251−1254.
3 Reiter, G. Unstable thin polymer films: rupture and dewetting processes. Langmuir 1993, 9(5), 1344−1351.
4 Reiter, G.; Sharma, A.; Casoli, A.; David, M.; Khanna, R.; Auroy, A. Thin film instability induced by long-range forces. Langmuir 1999, 15(7), 2551−2558.
5 Faldi, A.; Composto, R. J.; Winey, K. I. Unstable polymer bilayers. 1. morphology of dewetting. Langmuir 1995, 11(12), 4855−4861.
6 Qi, P.; Winey, K. I.; Hu, H. H.; Composto, R. J. Unstable polymer bilayers. 2. the effect of film thickness. Langmuir 1997, 13(6), 1758−1766.
7 Stange, T. G.; Evans, D. F.; Hendrickson, W. A. Nucleation and growth of defects leading to dewetting of thin polymer films. Langmuir 1997, 13(16), 4459−4465.
8 David, M. O.; Reiter, G.; Sitthaï T.; Schultz, J. Deformation of a glassy polymer film by long-range intermolecular forces. Langmuir 1998, 14(20), 5667−5672.
9 Safran, S. A.; Klein, J. Surface instability of viscoelastic thin films. J. Phys. B: At., Mol. Opt. Phys. 1993, 3(5), 749−757.
10 Wensink, K. D. F.; Jérôme B. Dewetting induced by density fluctuations. Langmuir 2002, 18(2), 413−416.
11 Reiter, G.; Hamieh, M.; Damman, P.; Sclavons, S., Gabriele, S.; Vilmin, T; Raphael, E. Residual stresses in thin polymer films cause rupture and dominate early stages of dewetting. Nat. Mater. 2005, 4(10), 754.
12 Kim, H. I.; Mate, C. M.; Hannibal, K. A.; Perry, S. S. How disjoining pressure drives the dewetting of a polymer film on a silicon surface. Phys. Rev. Lett. 1999, 82(17), 3496−3499.
13 Rittigstein, P.; Priestley, R. D.; Broadbelt, L. J.; Torkelson, J. M. Model polymer nanocomposites provide an understanding of confinement effects in real nanocomposites. Nat. Mater. 2007, 6(4), 278.
14 Desai, T.; Keblinski, P.; Kumar, S. K. Molecular dynamics simulations of polymer transport in nanocomposites. J. Chem. Phys. 2005, 122(13), 134910.
15 Alcoutlabi, M.; Mckenna, G. B. Effects of confinement on material behaviour at the nanometre size scale. J. Phys-Condense Mat. 2005, 17(15), R461−R524.
16 Mackay, M. E.; Tuteja, A.; Duxbury, P. M.; Hawker, C. J.; Horn, B. V.; Guan, Z.; Chen, G.; Krishnan, R. S. General

strategies for nanoparticle dispersion. Science 2006, 311(5768), 1740.
17 Balazs, A. C.; Emrick, T.; Russell, T. P. Nanoparticle polymer composites: where two small worlds meet. Science 2006, 314(5802), 1107−1110.
18 Ohno, K.; Morinaga, T.; Takeno, S.; Yoshinobu Tsujii, A.; Fukuda, T. Suspensions of silica particles grafted with concentrated polymer brush: effects of graft chain length on brush layer thickness and colloidal crystallization. Macromolecules 2007, 40(25), 9143−9150.
19 Wong, H. C.; Cabral, J. T. Spinodal clustering in thin films of nanoparticle-polymer mixtures. Phys. Rev. Lett. 2010, 105(3), 038301.
20 Barnes, K. A.; Karim, A.; Douglas, J. F.; Nakatani, A. I.; Gruell, H.; Amis, E. J. Suppression of dewetting in nanoparticle-filled polymer films. Macromolecules 2000, 33(11), 4177−4185.
21 Bandyopadhyay, D.; Douglas, J. F.; Karim, A. Influence of C60 nanoparticles on the stability and morphology of miscible polymer blend films. Macromolecules 2011, 20(20), 8136−8142.
22 Wong, H. C.; Cabral, J. T. Spinodal clustering in thin films of nanoparticle-polymer mixtures. Phys. Rev. Lett. 2010, 105(3), 038301.
23 Liu, T. X.; Phang, I. Y.; Lu, S.; And, S. Y. C.; Zhang, W. D. Morphology and mechanical properties of multiwalled carbon nanotubes reinforced nylon-6 composites. Macromolecules 2004, 37(19), 7214−7222.
24 Kim, B.; Lee, J.; Yu, I. Electrical properties of single-wall carbon nanotube and epoxy composites. J. Appl. Phys. 2003, 94(10), 6724−6728.
25 Che, J. Stability of polymer grafted nanoparticle monolayers: impact of architecture and polymerubstrate interactions on dewetting. ACS Macro Lett. 2016, 5(12), 1369−1374.
26 Che, J.; Park, K.; Grabowski, C. A.; Jawaid, A.; Kelley, J.; Koerner, H.; Vaia, R. A. Preparation of ordered monolayers of polymer grafted nanoparticles: impact of architecture, concentration, and substrate surface energy. Macromolecules 2016, 49(5), 1834−1847.
27 Ramanathan, T.; Abdala, A. A.; Stankovich, S.; Dikin, D. A.; Herrera-Alonso, M.; Piner, R. D.; Adamson, D. H.; Schniepp, H. C.; Chen, X.; Ruoff, R. S.; Nguyen, S. T.; Aksay, I. A.; Prud'Homme, R. K.; Brinson, L. C. Functionalized graphene sheets for polymer nanocomposites. Nat. Nanotechnol. 2008, 3(6), 327−331.
28 Potts, J. R.; Dreyer, D. R.; Bielawski, C. W.; Ruoff, R. S. Graphene-based polymer nanocomposites. Polymer 2011, 52(1), 5−25.
29 Cao, P.; Bai, P.; Omrani, A. A.; Xiao, Y.; Meaker, K. L.; Tsai, H. Z.; Yan, A.; Jung, H. S.; Khajeh, R.; Rodgers, G. F.; Kim, Y.; Aikawa, A. S.; Kolaczkowski, M. A.; Liu, Y.; Zettl, A.; Xu, K.; Crommie, M. F.; Xu, T. Preventing thin film dewetting *via* graphene capping. Adv. Mater. 2017, 29(36), 1701536.
30 Stankovich, S.; Piner, R. D.; Nguyen, S. B. T.; Ruoff, R. S. Synthesis and exfoliation of isocyanate-treated graphene oxide nanoplatelets. Carbon 2006, 44(15), 3342−3347.
31 Stankovich, S.; Dikin, D. A.; Dommett, G. H. B.; Kohlhaas, K. M.; Zimney, E. J.; Stach, E. A.; Piner, R. D.; Nguyen, S. T.; Ruoff, R. S. Graphene-based composite materials. Nature 2006, 442(7100), 282−286.
32 Chai, Y.; Salez, T.; Mcgraw, J. D.; Benzaquen, M.; Dalnoki-Veress, K.; Raphael, E.; Forrest, J. A. A direct quantitative measure of surface mobility in a glassy polymer. Science 2014, 343(6174), 994.
33 Zhu, Y.; Yang, Q.; You, J.; Li, Y. Composition fluctuation intensity effect on the stability of polymer films. RSC Adv. 2016, 6(74), 69715−69719.